Acceleration of snowmelt in an Antarctic Peninsula ice core during the 20th century

Nerilie J. Abram[1,2*], Robert Mulvaney[1], Eric W. Wolff[1], Jack Triest[1,3], Sepp Kipfstuhl[4], Luke D. Trusel[5], Françoise Vimeux[6], Louise Fleet[1] and Carol Arrowsmith[7]

1. British Antarctic Survey, Natural Environment Research Council, Cambridge CB3 0ET, United Kingdom.
2. Research School of Earth Sciences, The Australian National University, Canberra ACT 0200, Australia.
3. Laboratoire de Glaciologie et Géophysique de l'Environnement, Saint-Martin d'Hères, France.
4. Alfred Wegener Institute for Polar and Marine Research, D-27568 Bremerhaven, Germany.
5. Graduate School of Geography, Clark University, Worcester, MA, USA.
6. Institut de Recherche pour le Développement, Laboratoire HydroSciences Montpellier et Laboratoire des Sciences du Climat et de l'Environment, 91191 Gif-sur-Yvette, France.
7. NERC Isotope Geosciences Laboratory, British Geological Survey, Keyworth NG12 5GG, United Kingdom.
* e-mail: nerilie.abram@anu.edu.au

Antarctic Peninsula warming over the past 50 years has been accompanied by accelerating glacier mass loss and the retreat and collapse of ice shelves. A key driver in these ice losses is summer melting, however in Antarctic palaeotemperature reconstructions it is not usually possible to isolate the summer component that is critical for determining ice melt. Here we use visible melt layers in the James Ross Island ice core, alongside the deuterium temperature proxy, to reconstruct changes in mean temperature and ice melt intensity on the northern Antarctic Peninsula since 1000 AD. During the last millennium, the coolest conditions and lowest melt occurred between ~1410-1460 AD, when mean temperature was 1.6°C lower than in 1981-2000 AD. Over the same interval there has been a nearly ten-fold increase in melt intensity from 0.5% to 4.9%. While warming has occurred in progressive phases since ~1460 AD, most of the intensification of melting occurred since the mid-20th century and summer melting is now at a level that is unprecedented over the last 1000 years. This non-linear response highlights the particular vulnerability of the Antarctic Peninsula to rapid increases in melting and ice loss, even under scenarios of only small increases in mean temperature.

(NG edited first paragraph, 4 March 2013)

Over the past 50 years, warming of the Antarctic Peninsula has been accompanied by accelerating glacier mass loss and the retreat and collapse of ice shelves. A key driver of ice loss is summer melting, however it is not usually possible to specifically reconstruct the summer conditions that are critical for determining ice melt in the Antarctic. Here we reconstruct changes in mean temperature and ice melt intensity on the northern Antarctic Peninsula since AD1000, based on the identification of visible melt layers in the James Ross Island ice core and local mean annual temperature estimates from the deuterium content of the ice. During the past millennium, the coolest conditions and lowest melt occurred between about AD1410-1460, when mean temperature was 1.6 ^{o}C lower than that of 1981-2000. At the same time, there has been a nearly ten-fold increase in melt intensity from 0.5% to 4.9%. The warming has occurred in progressive phases since about AD1460, but intensification of melt is nonlinear, and has largely occurred since the mid-20th century. Summer melting is now at a level that is unprecedented over the last 1,000 years. We conclude that that Antarctic Peninsula region is now particularly susceptible to rapid increases in melting and ice loss in response to relatively small increases in mean temperature.

Over the last decade, satellite monitoring has revealed that mass loss from the margins of the Antarctic and Greenland ice sheets is more pervasive than previously realised and represents a significant source of sea level rise[1]. A key driver of accelerated glacier outflow on these ice sheet margins appears to be thinning and collapse of ice shelves. In some regions, such as the Amundsen Sea coast, ice shelf thinning is being driven by basal melting from warm marine waters[2]. On the Antarctic Peninsula, ice shelf instability and loss has instead been linked to an increase in surface melting due to higher air temperatures in summer[2-6]. Radar scatterometer data indicates that between 2000-2009 Antarctic Peninsula melt accounted for more than 50% of the total Antarctic surface melt intensity[7], a finding supported by regional climate modelling of surface meltwater production over 1979-2010[8].

Surface melting occurs in response to a positive energy balance after the snow surface temperature has warmed to its melting point. Several energy balance components critical to melt are strongly correlated with air temperature[9], and therefore the magnitude of above-freezing summer air temperatures is a well established proxy for melt intensity[10]. However, reconstructing the history of past summer temperature over Antarctica is difficult. Whilst stable isotope records from ice cores can provide quantified reconstructions of mean temperature, the isotopic diffusion[11,12] that occurs after snow deposition obscures the seasonal components except in the most highly resolved records. Instead, ice core records of melt can be used to gain information about past summer temperatures and surface snow melt, using either the occurrence of melt layers at sites where melt is rare[13-15] or the thickness of melt layers where melt occurs more frequently[16,17]. Such ice core melt records have been used to reconstruct the history of summer melting at various sites across the Arctic[15-17], however only one extended melt reconstruction so far exists for the Antarctic continent[14].

In this study, we measure the annual melt intensity preserved in the James Ross Island (JRI) ice core[18,19] and examine this alongside the ice core isotope record of mean temperature change over the last 1000 years. This first ice core reconstruction of melt history for the Antarctic Peninsula is particularly valuable as it is derived from the region (Fig 1a) where recent rapid atmospheric-warming[19,20] is hypothesised to have increased ice melt, leading to widespread ice shelf thinning and collapse[3-5,21-23] and accelerated glacier mass loss[24,25].

Evaluating the ice core proxies

The deuterium isotope (δD) composition of the JRI ice core is used as a proxy for mean annual temperature at the ice core site[18,19]. Previous assessments against meteorological reanalysis data since 1979 show that the isotope signal contains summer and winter temperature information and is not biased on seasonal or interannual time scales by snow accumulation[18]. The ice core δD record is significantly correlated with annual temperature measured at Esperanza Station ($r = 0.52$, $n = 56$, $p<0.0001$; Fig 1b). Esperanza is located close to sea level and approximately 100km north of the JRI ice core drill site. The mean annual temperature at Esperanza is -4.8°C, distributed around a winter (June-August) to summer (December-February) temperature range from -11.4°C to +0.9°C (1981-2000 interval). Based on borehole measurements, the temperature of the JRI ice cap at 10m depth is -13.8°C. This suggests that the mean annual temperature at JRI is on the order of 9°C lower than at Esperanza. Similarly, using the altitudinal lapse rate of -0.58°C per 100 metres observed on James Ross Island[26] and across the Antarctic Peninsula[27] indicates that the ice core site at 1524m elevation should be approximately 8.9°C lower than sea level temperature in the area.

In order to examine how variability of melt intensity in the JRI ice core relates to positive summer temperatures we used daily observations of maximum temperature from Esperanza Station[28]. We applied a -9°C offset to the Esperanza daily temperature data as a first-order estimate of the temperature difference between the ice core site and Esperanza, before calculating the annual (July-June) sum of all daily temperatures exceeding 0°C, known as the positive degree-day sum (PDD)[13,14,29]. Because the PDD parameter is based on a cumulative sum of daily temperatures we required daily data coverage greater than 90% during the summer months (December-February), resulting in many years where a reliable estimation of PDD was not possible. The mean of positive daily temperatures is a less precise parameter for describing melt than the PDD sum, but it is not systematically biased to lower values by missing data. Thus the mean of daily temperatures exceeding $0^{o}C$ (PD mean) in the Esperanza station data was also used as a more continuous observational record to compare with melt at JRI.

Visual melt layers in the JRI ice core were used to calculate melt intensity as the percentage of the annual water-equivalent accumulation that melted and refroze (Methods). The average melt intensity at JRI was 4.9% during the 1981-2000 interval, with a maximum annual melt of 18% recorded in the JRI ice core during the 1997/98 summer (Fig. 1c). The annual percentage of melt at JRI has a significant positive correlation with PDDs calculated using the Esperanza station data ($r = 0.64$, $n=32$, $p=0.0001$). A clear correlation also exists between the PD mean and annual melt ($r = 0.53$, $n=43$, $p=0.0003$), as well as in their interannual variability illustrated by 5-year moving averages (Fig. 1d).

Further verification of the JRI melt record comes from its comparison with QuikSCAT radar scatterometer monitoring of melting[7]. Although the scatterometer data only offer a short interval of overlap with the JRI record (2000-2007), they give continuous data coverage over this time and, unlike other longer satellite-derived melt records, they are sufficiently well-resolved (effectively 8-10 km resolution)[7] to isolate a melt signal for the summit of the JRI ice cap. The scatterometer data for JRI show that melt occurs at this site between October and March and is concentrated in the December-February summer months. Although the sample size is small, annual variability in scatterometer-derived melt is significantly correlated with melt intensity in the JRI ice core ($r = 0.81$, $n = 7$, $p = 0.027$; Fig. 1c) and, together with the Esperanza station data, confirms that the JRI ice core-melt record is representative of summer warmth inducing melt at this site.

Antarctic Peninsula climate during the 20th century

To first characterise the spatial patterns of climate variability in this region, the JRI δD record of mean annual temperature was examined alongside similar annually-resolved ice core temperature records from the Antarctic Peninsula and the West Antarctic Ice Sheet[30,31]. Using principal component (PC) analysis, the two leading modes of the ice core array since 1900 AD highlight differences between recent warming on the West Antarctic Ice Sheet and the Antarctic Peninsula (Fig. 2). PC1 is the West Antarctic climate signal that is well-documented for its significant warming in winter and spring[32-34], and more recently has been shown to also have a significant component of summer warming[35]. Warming in this region has been attributed to increased advection of warm airmasses onto continental West Antarctica caused by strengthening teleconnections with Pacific Ocean climate variability, focussed particularly in the subtropical South Pacific Convergence Zone[30,32-35] (Supplementary Figure 1). The recent phase of warming over the West Antarctic Ice Sheet has been ongoing since the 1950s (Fig. 2c)[35], although with the length-constraints of the current ice core records it is not possible to determine if the strong multi-decadal variability in PC1 masks an earlier inception of the warming trend over the West Antarctic Ice Sheet. Recently, borehole temperature estimates from the West Antarctic Ice Sheet have provided evidence for a rapid acceleration of West Antarctic warming over the last two decades[36].

Antarctic Peninsula warming is captured by PC2 of the ice core array (Fig. 2). The spatial composition of PC2 transitions from a strong positive contribution at JRI on the northern Antarctic Peninsula to a negative component on the Ross Sea side of West Antarctica. Correlation of PC2 with ERA-Interim[37] 2m temperature confirms this spatial pattern with opposing temperature anomalies focused over the Weddell and Amundsen-Ross sea regions (Fig. 3c). The correlation of PC2 with ERA-Interim sea level pressure indicates that this temperature pattern is associated with pressure anomalies over the Antarctic continent and Amundsen Sea which are of opposite sign to the pressure anomalies within the mid-latitude band (Fig. 3b). This pressure pattern is characteristic of Southern Annular Mode (SAM)[38] circulation around the Antarctic continent, and is the leading mode of Southern Hemisphere climate variability in the ERA-Interim reanalysis since 1979 (Supplementary Figure 2). The role of the SAM on Antarctic Peninsula temperature variability during the 20th century is further demonstrated by significant correlations of historical reconstructions of the SAM index[38,39] with PC2 from the ice core array and the JRI mean annual temperature record (Supplementary Table 1; Fig. 3a). These correlations are strongest during the summer and autumn seasons.

The length of the JRI temperature reconstruction allows for a statistical assessment of when the recent rapid warming of the Antarctic Peninsula was initiated. We examined this by filtering the 1000-year annual temperature reconstruction across a range of filter widths to assess the significance of temperature trends in the record at different levels of smoothing[40] (Fig. 4, Methods). The inflection point of all filters between 15-40 year bandwidths indicates that the recent warming trend at JRI began around the 1920s (1928 ± 6 years; 2σ) and has been statistically significant (exceeding 90% confidence) since the 1940s (1942 ± 4 years). This warming is seen simultaneously in mean annual temperature and summer-melt intensity (Fig. 3a), suggesting a persistent summer component to Antarctic Peninsula warming during the 20th century. These findings are in agreement with nearby station data indicating that warming at Orcadas (the only Antarctic site where climate observations span more than 100 years)[41] has been significant since ~1950, and has been particularly strong in summer and autumn[42].

Circulation changes associated with stratospheric ozone depletion have been widely discussed as a driver of summer strengthening of the SAM and associated recent warming on the Antarctic Peninsula[43]. However, the mid-20th century start for significant warming of the Antarctic Peninsula is too early to be explained by the ozone depletion mechanism alone, and suggests that the early warming was influenced by other factors such as rising greenhouse gas concentrations or natural variability that has since been reinforced by ozone depletion-driven circulation changes[41,44]. Our new constraints for the timing of recent warming at JRI will provide a valuable dataset for assessing the ability of current climate models run under realistic transient forcings (including the Coupled Model Intercomparison Project Phase 5 (CMIP5) experiments) to simulate the 20th century progression of Antarctic Peninsula warming.

Temperature and ice melt over the last millennium

The coolest conditions at JRI over the last millennium occurred between ~1410-1460 AD, when mean temperature was 1.6^{o}C lower than the 1981-2000 interval (Fig. 4). Warming since this time has occurred in progressive phases (Fig. 4b). As well as the warming since the mid-20th century, two intervals of significant warming also occurred between ~1550-1600 AD and ~1710-1760 AD.

The JRI ice core melt record has its minimum melt intensity for the last millennium between ~1410-1460 AD, coinciding with the coolest interval in mean annual temperature (Fig. 5). At this time summer ice melt at JRI made up only 0.5% of the total accumulation. This represents a roughly 10-fold lower melt intensity compared with the 4.9% melt observed for 1981-2000 AD.

The history of melt intensity at JRI has visual similarities with the reconstruction of melt occurrence at Siple Dome[14] on the West Antarctic Ice Sheet (Figs. 1a & 5d). Both reconstructions show particularly low melt in the early 15th century, and that prior to the 20th century the highest summer melting occurred during the 16th century. Interestingly, the 16th century is not characterised by similar warmth in the JRI mean annual temperature reconstruction, and borehole temperature information indicates that this was broadly a cool interval in West Antarctica[36]. This implies that the high levels of melt on the Antarctic Peninsula and West Antarctic Ice Sheet during the 16th century were caused by an increased annual temperature range or increased interannual variability (i.e. increased occurrence of warm summers and cool winters) rather than a warmer mean climate state.

The increase in summer melting at Siple Dome during the 20th century is not as pronounced as at JRI. The Siple Dome record does not provide information on any melt that may have occurred since the ice core was drilled in 1999, so does not include a full response to the acceleration of West Antarctic warming in the last 20 years[36]. However, the frequency of melt during the 20th century (3 melt events) was clearly less than the melt frequency at this site during the 16th century (7 melt events). The principal component analysis of spatial temperature variability during the 20th century (Fig. 3, Supplementary Fig. 2) indicated that the summer strengthening of the SAM that has caused at least part of the warming at the JRI site is also likely to have suppressed the rate of summer warming and melting (relative to strong winter and spring warming) in the Siple Dome region[35]. Nevertheless, statistically significant summer warming of the West Antarctic Ice Sheet has now been detected which is increasing the probability of future surface melting across the region[35].

The most striking difference between the mean annual temperature and melt histories from the JRI ice core over the last 1000 years is the non-linear characteristic of melt (Fig. 5). Mean annual temperature shows phases of progressive warming from ~1460 AD to present day superimposed upon a high degree of interannual to multidecadal variability, and the rate of warming over the last century has been shown to be highly unusual but not unprecedented in the context of natural climate variability[19]. In contrast, the JRI melt history shows more muted decadal-scale variability and its dominant feature over the last millennium is instead a sharp intensification since the mid-20th century to levels of melt that are unprecedented within the last 1000 years.

The non-linear response of melt to changes in mean temperature at JRI can be explained by the ~0^{o}C threshold of melting, meaning that in cooler conditions the ice melt record loses the ability to record variability in the surface energy balance and, by extension, summer temperatures. In addition, where summer temperatures do exceed the melting threshold, the amount of melt produced is proportional to the sum of the daily positive temperatures rather than their mean[7,13]. This means that as average summer temperature increases and positive temperature days become warmer and more frequent, the amount of melt produced will exhibit an exponential increase[29,45] (Supplementary Fig. 3). The strong summer component of 20th century warming on the Antarctic Peninsula also appears to have been critical in driving the unprecedented levels of melt here in recent decades, as the current mean annual temperature at JRI is not unprecedented within the scale of decadal variability at the site (Figs. 3 & 5).

The combined JRI ice core record of mean annual temperature and melt intensity provides a clear demonstration from the palaeoclimate record of the potential in the polar regions for non-linear responses to future climate change. The non-linearity of melt can help to explain how the relatively modest lowering of mean temperature at JRI in the late Holocene was sufficient to enable the establishment of a permanent ice shelf in Prince Gustav Channel[19,23], and also why this ice shelf apparently underwent rapid retreat and disintegration in the late 20th century[21,23] rather than gradual retreat during the centuries of progressive warming since ~1460 AD (Fig. 5a). The non-linearity of melt observed in the JRI ice core record also highlights the particular vulnerability of areas in the polar regions where daily maximum temperatures in summer are close to 0°C and/or where summer isotherms are widely-spaced, such as along the east and west coasts of the Antarctic Peninsula (Supplementary Fig. 3). In these places even modest future increases in mean atmospheric temperature could translate into rapid increases in the intensity of summer melt and in the poleward extension of areas where glaciers and ice shelves are undergoing decay caused by atmospheric-driven melting.

Methods

The James Ross Island (JRI) ice core was drilled 363.9 m to bedrock in January-February 2008 at 057°41.10'W, 64°12.10'S. Elevation at this site is 1524 m, and mean water-equivalent accumulation is 0.63 m y^{-1} (refs. 18,19). The upper 200 years of the ice core chronology is based on annual layer counting, using the well-defined annual cycle in non-sea salt SO_4 (ref. 18). The annual layer age scale is also constrained by fixed-time markers; a tephra layer from the 1967 Deception Island eruption, and the global SO_4 anomalies of the 1815 Tambora and 1809 Unknown eruptions[18,19]. Beyond 1807 AD the age scale used here is the JRI-1 age scale, based on a glaciological flow model for the JRI site with an additional offset derived from 14 tephra horizons and the 1259 AD volcanic sequence[19]. The 1259 AD marker has an estimated uncertainty of ± 5 years and provides a firm age constraint for the last millennium of the JRI record that is examined here.

Analytical details for the measurement of the deuterium isotope (δD) profile of the JRI core are described fully in Mulvaney et al., (ref 19). Analytical precision on the δD measurements is typically 1.0 ‰. The JRI δD data were averaged into annual bins to produce a record of mean δD in the ice core since 1000 AD. Annual bins for the isotope data run from January-December and were selected to facilitate comparison with similar calendar-year annual isotope records from West Antarctic ice cores. A temperature dependence of 6.4 ‰ $^{o}C^{-1}$ was used to derive a temperature history from the δD record at this site[18]. Temperature anomalies are calculated with respect to 1981-2000 AD, that coincides with the time of rapid retreat and collapse of the adjacent Prince Gustav ice shelf[21]. Consistent temperature results are also produced by using $\delta^{18}O$ measured in the JRI ice core[18,19]. An analysis of temperature trends over the last 1000 years was carried out using the SiZer (SIgnificant ZERo crossings of derivatives) method[40] to calculate the significance of trends across different levels of smoothing. Smoothing was performed using a Gaussian kernel filter with bandwidths spanning all integer years in the range from 5 to 50 years. Assessments of the timing for the initiation of the 20th century warming trends use the mean and standard deviation of the changepoints in all filters between 15-40 years bandwidth so as to reduce the effect of high frequency (interannal to decadal) variability on the change point estimates. The SiZer program was obtained at http://www.unc.edu/~marron/marron_software.html

The presence and thickness of melt layers in the JRI ice core was determined using linescan images of the core that were measured on the surface of 55 cm long, 9.8 cm wide, and 3.3 cm thick slabs cut during ice core processing at Alfred Wegener Institute. The images were analysed for melt layers using a custom-built program in LabView software. To meet the classification of a melt layer[13,14], the melt feature had to be a layer of bubble-free ice with a sharp lower boundary that extended across at least 50% of the width of the core. Melt layers were common features in the ice core, although signs of large scale melt percolation such as vertical melt pipes were not observed in the linescan images. Supplementary figure 4 gives examples of line scan images and melt assignment for three core pieces representing the near surface, mid depth and deep portions of the melt record.

Melt layers were picked from the surface to a depth of 302.4 m. Beyond this melt layers are still evident in the linescan images of the JRI ice core, however thinning of the annual ice layers by this depth made it uncertain that all layers would still be reliably detected. In this paper we present the melt layer data back to 1000 AD, which corresponds to a depth of 283.2 m in the JRI ice core and an annual layer thickness of 7.1 cm based on the JRI-1 chronology[19]. The position and thickness of the melt layers were used to calculated the percentage of the summer-centred (July-June) annual accumulation that was comprised of melt after conversion of both parameters to water-equivalent lengths[17]. Water equivalence of annual snow layers used a snow-water depth conversion based on density measurements along the length of the core, and for melt width used the 0.917 g cm^{-3} density of ice. Expressing melt as a percentage relative to annual accumulation, and assuming that ice sheet thinning with depth affects melt layers in the same way as the annual water-equivalent layers, removes the need to apply a thinning correction to the melt thickness data[17] which is desirable as thinning corrections become more uncertain with depth down an ice core. There is no long-term trend or deviation in the thinning-corrected annual accumulation at the JRI site over the 200 years spanning the annual chronology of the JRI core, indicating that the 20th century intensification of melt is not affected by its expression relative to annual layer thickness. An alternative method of quantifying melt (independently of annual layer thickness) as the annual sum of melt thickness adjusted for thinning using the Nye equation[46] confirms that the results obtained for annual melt percentage are robust (Supplementary figure 5).

The ice core deuterium and melt data used in this study have been archived with the World Data Centre for Paleoclimatology Data[47].

Acknowledgements

We thank our colleagues in the field, Olivier Alemany, Susan Foord, Samantha Shelley, and Louise Sime, who took part in the ice core drilling project; the Captain and crew of HMS Endurance who provided logistical support for the drilling field season; Susan Foord, Nicola Lang, James Levine, Louise Sime, Regine Rothlisberger, and the Alfred Wegner Institute at Bremerhaven for assistance in the processing of the ice core; and Emilie Capron, Susan Foord and Emily Ludlow for laboratory assistance. This study was aided by the use of the KNMI Climate Explorer web resource provided by Geert Jan van Oldenborgh, and we thank Sarah Das, Hamish Pritchard, John King and Claire Krause for helpful discussions during the preparation of the manuscript. This study is part of the British Antarctic Survey Polar Science for Planet Earth Programme, and was funded by the Natural Environment Research Council. Support from the Institut Polaire Français - Paul Emile Victor and the Institut National des Sciences de l'Univers in France, facilitated by Jerome Chappellaz and Françoise Vimeux, enabled the technical contribution of the French National Center for Drilling and Coring (INSU/C2FN). Nerilie Abram is supported by a Queen Elizabeth II fellowship awarded by the Australian Research Council (DP110101161).

Author Contributions

RM led the team to drill the ice core, that also involved NJA and JT; JT and SK performed the linescan measurements and JT wrote the Labview software for melt analysis; NJA and JT performed the melt layer analysis; NJA, RM, LF and CA performed the chemical analysis; NJA and RM developed the ice core age scale; LT provided satellite melt data for JRI; NJA led the data analysis and wrote the paper with contributions from RM, EWW, LT and FV.

Additional Information

Supplementary Information is available in the online version of the paper. Reprints and permissions information is available online at www.nature.com/reprints. Correspondence and requests for materials should be addressed to NJA (nerilie.abram@anu.edu.au) and RM (rmu@bas.ac.uk).

Additional Information

The authors declare no competing financial interests.

References

1 Pritchard, H. D., Arthern, R. J., Vaughan, D. G. & Edwards, L. A. Extensive dynamic thinning on the margins of the Greenland and Antarctic ice sheets. *Nature* **461**, 971-975, doi:10.1038/nature08471 (2009).

2 Pritchard, H. D. *et al.* Antarctic ice-sheet loss driven by basal melting of ice shelves. *Nature* **484**, 502-505, doi:10.1038/nature10968 (2012).

3 Scambos, T. *et al.* Ice shelf disintegration by plate bending and hydro-fracture: Satellite observations and model results of the 2008 Wilkins ice shelf break-ups. *Earth Plant. Sci. Lett.* **280**, 51-60, doi:10.1016/j.epsl.2008.12.027 (2009).

4 Scambos, T. A., Hulbe, C., Fahnestock, M. & Bohlander, J. The link between climate warming and break-up of ice shelves in the Antarctic Peninsula. *J. Glacio.* **46**, 516-530, doi:10.3189/172756500781833043 (2000).

5 van den Broeke, M. Strong surface melting preceded collapse of Antarctic Peninsula ice shelf. *Geophys. Res. Lett.* **32**, L12815, doi:10.1029/2005gl023247 (2005).

6 Barrand, N. E. *et al.* Trends in Antarctic Peninsula surface melting conditions from observations and regional climate modelling. *J. Geophys. Res.*, doi:10.1029/2012JF002559 (2013).

7 Trusel, L. D., Frey, K. E. & Das, S. B. Antarctic surface melting dynamics: Enhanced perspectives from radar scatterometer data. *J. Geophys. Res.* **117**, F02023, doi:10.1029/2011JF002126 (2012).

8 Kuipers Munneke, P., Picard, G., van den Broeke, M. R., Lenaerts, J. T. M. & van Meijgaard, E. Insignificant change in Antarctic snowmelt volume since 1979. *Geophys. Res. Lett.* **39**, L01501, doi:10.1029/2011GL050207 (2012).

9 Hock, R. Temperature index melt modelling in mountain areas. *J. Hydrology* **282**, 104-115, doi:10.1016/S0022-1694(03)00257-9 (2003).

10 Ohmura, a. Physical basis for the temperature-based melt-index method. *J App. Meteorology* **40**, 753-761, doi:doi:10.1175/1520-0450(2001)040<0753:PBFTTB>2.0.CO;2 (2001).

11 Cuffey, K. M. & Steig, E. J. Isotopic diffusion in polar firn: implications for interpretation of seasonal climate parameters in ice-core records, with emphasis on central Greenland. *J. Glacio.* **44**, 273-284 (1998).

12 Johnsen, S. J. *et al.* in *Physics of Ice Core Records* (ed T. Hondoh) 121-140 (Hokkaido University Press, 2000).

13 Das, S. B. & Alley, R. B. Characterization and formation of melt layers in polar snow: Observations and experiments from West Antarctica. *J. Glacio.* **51**, 307-312, doi:10.3189/172756505781829395 (2005).

14 Das, S. B. & Alley, R. B. Rise in frequency of surface melting at Siple Dome through the Holocene: Evidence for increasing marine influence on the climate of West Antarctica. *J. Geophys. Res.* **113**, D02112, doi:10.1029/2007jd008790 (2008).

15 Alley, R. B. & Anandakrishnan, S. Variations in melt-layer frequency in the GISP2 ice core: implications for Holocene summer temperatures in central Greenland. *Ann. Glaciol.* **21**, 64-70 (1995).

16 Fisher, D. *et al.* Recent melt rates of Canadian arctic ice caps are the highest in four millennia. *Glob. Plan. Change* **84-85**, 3-7 (2012).

17 Herron, M. M., Herron, S. L. & Langway Jr, C. C. Climatic signal of ice melt features in southern Greenland. *Nature* **293**, 389-391 (1981).

18 Abram, N. J., Mulvaney, R. & Arrowsmith, C. Environmental signals in a highly resolved ice core from James Ross Island, Antarctica. *J. Geophys. Res.* **116**, D20116, doi:10.1029/2011jd016147 (2011).

19 Mulvaney, R. *et al.* Recent Antarctic Peninsula warming relative to Holocene climate and ice-shelf history. *Nature* **489**, 141-144 (2012).

20 Vaughan, D. G. *et al.* Recent rapid regional climate warming on the Antarctic Peninsula. *Climatic Change* **60**, 243-274 (2003).
21 Cooper, A. P. R. Historical observations of Prince Gustav Ice Shelf. *Polar Rec.* **33**, 285-294 (1997).
22 Domack, E. *et al.* Stability of the Larsen B ice shelf on the Antarctic Peninsula during the Holocene epoch. *Nature* **436**, 681-685, doi:10.1038/nature03908 (2005).
23 Pudsey, C. J., Murray, J. W., Appleby, P. & Evans, J. Ice shelf history from petrographic and foraminiferal evidence, Northeast Antarctic Peninsula. *Quat. Sci. Rev.* **25**, 2357-2379 (2006).
24 Cook, A. J., Fox, A. J., Vaughan, D. G. & Ferrigno, J. G. Retreating glacier fronts on the Antarctic Peninsula over the past half-century. *Science* **308**, 541-544 (2005).
25 Kunz, M. *et al.* Multi-decadal glacier surface lowering in the Antarctic Peninsula. *Geophys. Res. Lett.* **39**, L19502, doi:10.1029/2012GL052823 (2012).
26 Aristarain, A. J., Pinglot, J. F. & Pourchet, M. Accumulation and temperature measurements on the James Ross Island ice cap, Antarctic Peninsula, Antarctica. *J. Glacio.* **33**, 357-362 (1987).
27 Reynolds, J. M. Distribution of mean annual temperatures in the Antarctic Peninsula. *British Antarctic Survey Bulletin* **54**, 123-133 (1981).
28 Tank, K. Daily dataset of 20th-century surface air temperature and precipitation series for the European Climate Assessment. *Int. J. Clim.* **22**, 1441-1453 (2002).
29 Braithwaite, R. J. in *Encyclopedia of snow, ice and glaciers* (eds V.P. Singh, P. Singh, & U.K. Haritashya) (Springer, 2011).
30 Schneider, D. P. & Steig, E. J. Ice cores record significant 1940s Antarctic warmth related to tropical climate variability. *Proc. Nat. Acad. Sci.* **105**, 12154-12158, doi:10.1073/pnas.0803627105 (2008).
31 Thomas, E. R., Dennis, P. F., Bracegirdle, T. J. & Franzke, C. Ice core evidence for significant 100-year regional warming on the Antarctic Peninsula. *Geophys. Res. Lett.* **36**, L20704, doi:10.1029/2009GL040104 (2009).
32 Ding, Q. H., Steig, E. J., Battisti, D. S. & Kuttel, M. Winter warming in West Antarctica caused by central tropical Pacific warming. *Nature Geosci.* **4**, 398-403, doi:10.1038/ngeo1129 (2011).
33 Schneider, D. P., Deser, C. & Okumura, Y. An assessment and interpretation of the observed warming of West Antarctica in the austral spring. *Clim. Dynam.* **38**, 323-347, doi:10.1007/s00382-010-0985-x (2012).
34 Steig, E. J. *et al.* Warming of the Antarctic ice-sheet surface since the 1957 International Geophysical Year. *Nature* **457**, 459-U454, doi:10.1038/nature07669 (2009).
35 Bromwich, D. H. *et al.* Central West Antarctica among the most rapidly warming regions on Earth. *Nature Geosci.* **6**, 139-144, doi:10.1038/ngeo1671 (2013).
36 Orsi, A. J., Cornuelle, B. D. & Severinghaus, J. P. Little Ice Age cold interval in West Antarctica: Evidence from borehole temperature at the West Antarctic Ice Sheet (WAIS) Divide. *Geophys. Res. Lett.* **39**, L09710, doi:10.1029/2012GL051260 (2012).
37 Berrisford, P. *et al.* The ERA-Interim archive. 16 (Reading UK, 2009).
38 Marshall, G. J. Trends in the southern annular mode from observations and reanalyses. *J. Clim.* **16**, 4134-4143 (2003).
39 Fogt, R. L. *et al.* Historical SAM Variability. Part II: Twentieth-Century Variability and Trends from Reconstructions, Observations, and the IPCC AR4 Models. *J. Clim.* **22**, 5346-5365, doi:10.1175/2009jcli2786.1 (2009).
40 Chaudhuri, P. & Marron, J. S. SiZer for exploration of structure in curves. *J. Am. Stat. Assoc.* **94**, 807-823 (1999).
41 Zazulie, N., Rusticucci, M. & Solomon, S. Change in climate at high southern latitudes: a unique daily record at Orcadas spanning 1903-2008. *J. Clim.* **23**, 189-196, doi:10.1175/2009JCLI3074.1 (2010).

42 Marshall, G. J., Orr, A., van Lipzig, N. P. M. & King, J. C. The impact of a changing Southern Hemisphere Annular Mode on Antarctic Peninsula summer temperatures. *J. Clim.* **19**, 5388-5404 (2006).
43 Thompson, D. W. J. & Solomon, S. Interpretation of Recent Southern Hemisphere Climate Change. *Science* **296**, 895-899, doi:10.1126/science.1069270 (2002).
44 Marshall, G. J. *et al.* Causes of exceptional atmospheric circulation changes in the Southern Hemisphere. *Geophys. Res. Lett.* **31**, L14205, doi:10.1029/2004GL019952 (2004).
45 Vaughan, D. G. Recent trends in melting conditions on the Antarctic Peninsula and their implications for ice-sheet mass balance and sea level. *Arct. Antarct. Alp. Res.* **38**, 147-152, doi:10.1657/1523-0430(2006)038[0147:rtimco]2.0.co;2 (2006).
46 Nye, J. F. Correction factor for accumulation measured by the thickness of the annual layers in an ice sheet. *J. Glacio.* **4**, 785-788 (1963).
47 Abram, N. J. *et al.* James Ross Island ice core 1000 year deuterium and melt data. IGBP PAGES/World Data Centre for Paleoclimatology Data, (2013). ftp://ftp.ncdc.noaa.gov/pub/data/paleo/icecore/antarctica/james-ross-island/

Figure captions

Figure 1. Location and proxies. a, JRI lies near the northeastern tip of the Antarctic Peninsula. b, Mean annual (Jan-Dec) δD of the JRI ice core (green) and mean annual temperature at Esperanza (black). c, Annual (Jul-Jun) melt percentage at JRI (red), alongside QuikSCAT melt decibel-days for the JRI site (MDD; sum of backscatter exceeding melt threshold; cyan)[7], and Esperanza annual positive degree day sum (PDD; black, daily data adjusted by -9^{o}C). d, as in (c) but using positive degree day mean (PD mean; black). Dashed lines show 1981-2000 ice core means (b-d), bold curves are 5-year running means (d).

Figure 2. Antarctic Peninsula and West Antarctic Ice Sheet warming. a, Mean annual (Jan-Dec) temperature reconstructions for JRI (green), Gomez (cyan)[31], and a West Antarctica ice core stack (ITASE 01-5, 01-3, 01-2, 00-1 and 00-5; blue)[30]. Anomalies relative to 1981-2000 mean (dashed lines), thick curves are 11-year running means. b, The seven ice core locations and their loadings for, c, the two leading modes of variability determined by PC analysis. PC1 (grey) is focused over West Antarctica, while PC2 (black) has a strong positive sign on the Antarctic Peninsula transitioning to negative on the Ross Sea side of West Antarctica.

Figure 3. Antarctic Peninsula climate variability. a, Mean annual (Jan-Dec) JRI temperature (green) and PC2 of the Antarctic Peninsula/West Antarctic ice core array (black) correlate with the SAM index in summer and autumn (Marshall, dark blue[38]; Fogt, light blue[39]; Dec-May averages shown). The annual (Jul-Jun) percentage of melt at JRI (red) increases coincident with 20th century warming. Thick lines show 11-year running means, dashed lines denote 1981-2000 means. The spatial correlation of PC2 with ERA-Interim[37], b, MSLP and c, 2m-temperature (Jan-Dec annuals) supports SAM as a driver of the PC2 spatial temperature pattern. Dark shading shows correlations exceeding 90% confidence.

Figure 4. Antarctic Peninsula temperature over the last millennium. a, 11-year moving average of JRI annual temperature (green) with Gaussian kernel smoothing filters at 5, 10, 20, 30, 40, and 50-year bandwidths (grey). A 21-year filter (black) provides the best data-driven filtering length determined using b, SiZer[40] to examine the significance of temperature trends across different filter lengths. Positive (negative) trends are shown by red (blue) shading, and dark shading indicates trends exceeding 90% confidence. Vertical dashed line denotes the start of 20th century warming across 15-40 year filter widths (1928 ± 6 years (2σ)).

Figure 5. Melt response over the last millennium. a, Schematic of Prince Gustav ice shelf history showing its presence (blue), intervals of rapid retreat (1957 and 1989; yellow), and collapse (1995; red)[21,23]. b, JRI mean temperature anomalies (green) and c, melt percentage (red) shown as 11-year moving averages. Thick lines are 21-year Gaussian kernel filters, dashed lines denote 1981-2000 mean. Lowest temperatures and melt occurred at ~1410-1460 AD, followed by progressive warming

and a non-linear melt increase. d, The occurrence of melt layers (grey lines) and a 100-year stepped average of melt frequency (purple) at Siple Dome[14] in West Antarctica.

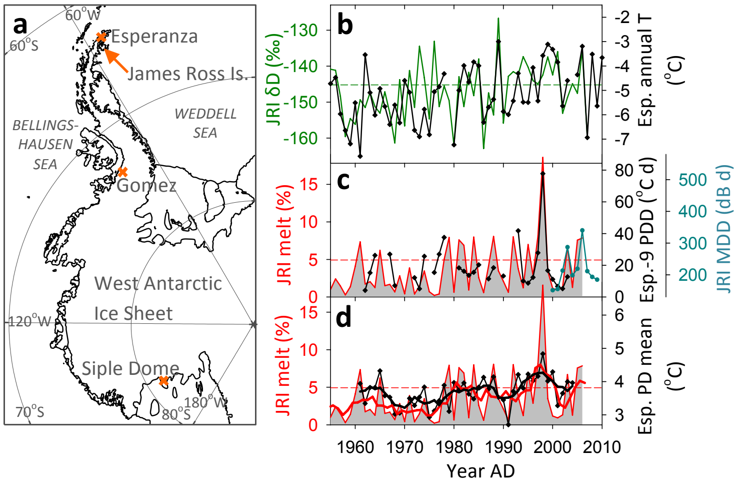

a
60°W
60°S
Esperanza
James Ross Is.
BELLINGS-
HAUSEN
SEA
WEDDELL
SEA
Gomez
West Antarctic
Ice Sheet
120°W
Siple Dome
70°S
80°S
180°W
b
JRI δD (‰)
Esp. annual T (°C)
c
JRI melt (%)
Esp.-9 PDD (°C d)
JRI MDD (dB d)
d
JRI melt (%)
Esp. PD mean (°C)
Year AD

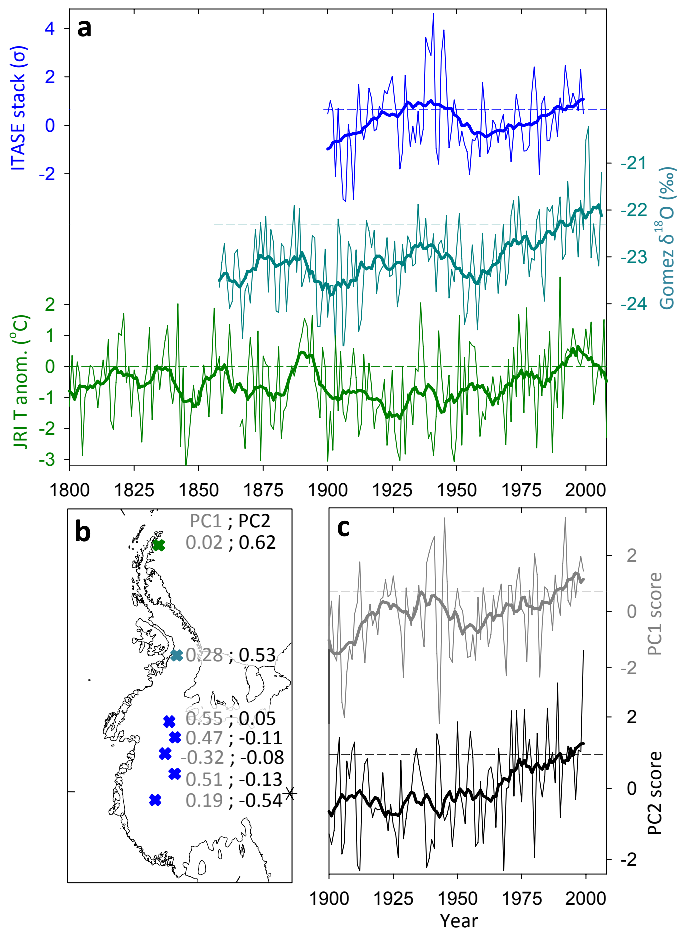

a
ITASE stack (σ)
Gomez δ18O (‰)
JRI T anom. (°C)
1800
1825
1850
1875
1900
1925
1950
1975
2000
b
PC1 ; PC2
0.02 ; 0.62
0.28 ; 0.53
0.55 ; 0.05
0.47 ; -0.11
-0.32 ; -0.08
0.51 ; -0.13
0.19 ; -0.54
c
PC1 score
PC2 score
Year

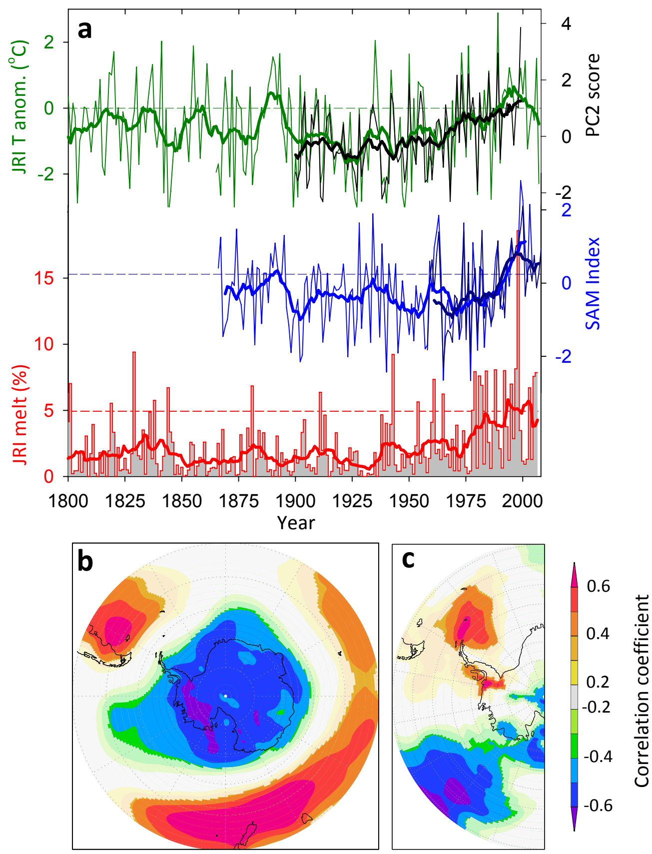

a
JRI T anom. (°C)
PC2 score
SAM Index
JRI melt (%)
1800
1825
1850
1875
1900
1925
1950
1975
2000
Year
b
c
0.6
0.4
0.2
-0.2
-0.4
-0.6
Correlation coefficient

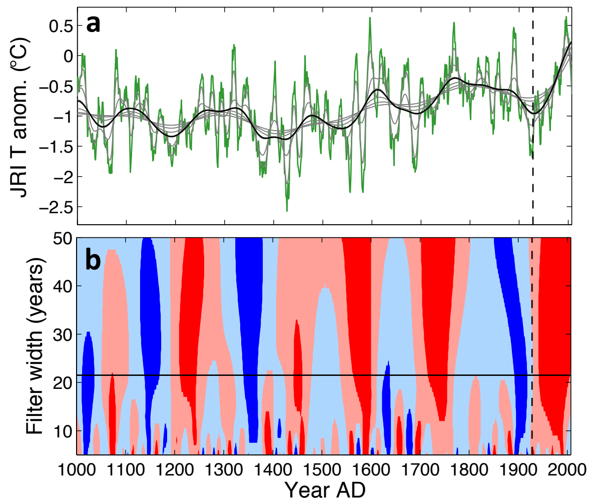

a
JRI T anom. (°C)
0.5
0
-0.5
-1
-1.5
-2
-2.5
b
Filter width (years)
50
40
30
20
10
1000
1100
1200
1300
1400
1500
1600
1700
1800
1900
2000
Year AD

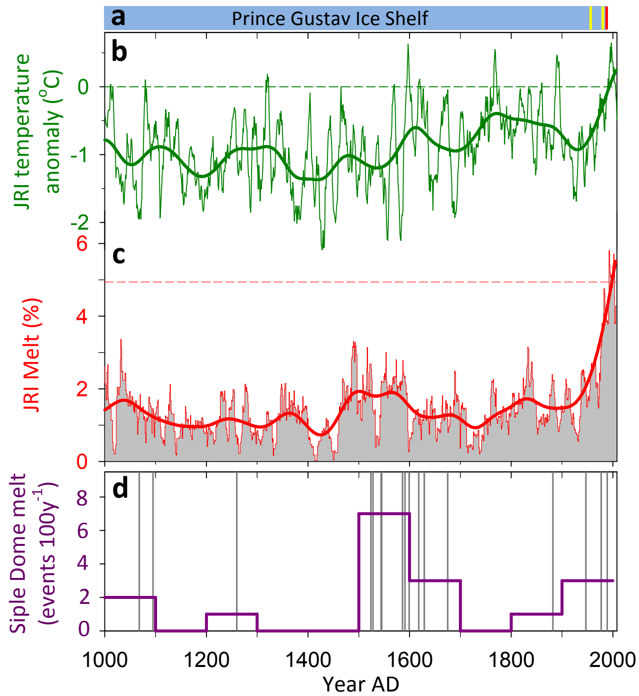

a
Prince Gustav Ice Shelf
b
JRI temperature anomaly (°C)
0
-1
-2
c
JRI Melt (%)
6
4
2
0
d
Siple Dome melt (events 100y-1)
8
6
4
2
0
1000
1200
1400
1600
1800
2000
Year AD